APPLICATION OF VISCOUS-INVISCID INTERACTION METHODS FOR A SEPARATED FLOW CALCULATION ABOUT AIRFOILS AND HIGH-LIFT SYSTEMS

S.V.Lyapunov, A.V.Wolkov
Central Aerohydrodynamics Institute (TsAGI)
Zhukovsky, Moscow region, Russia

Abstract

An approach is considered for calculation of steady attached and separated 2D flows. The approach is based on viscous-inviscid interaction model. A quasi-simultaneous method of viscous-inviscid coupling is used with a specific boundary condition for an inviscid flow when separation occurs. This approach is proved to be rapidly convergent both for attached and separated flows. Two computer codes based on this approach are developed. The first code - VISTRAN - permits one to calculate a transonic flow about single airfoil, the second one - MULTIVIS - to calculate a subsonic flow about multi-element high-lift systems. Calculation of outer (inviscid) flow is carried out by panel method for low speeds or by a solution of a modified transonic potential equation for high subsonic speeds. Inner (viscous) flow is described by laminar and turbulent boundary layer equations in an integral form. In the regions of pre-separated and separated flow these equations are solved in an inverse mode in order to avoid the Goldstein singularity in the separation and reattachment points. Calculated results show good agreement with experimental results both for single and multi-element cases including determination of maximum lift and its dependence on Mach and Reynolds numbers as well as on flap deflection for high-lift systems.

Introduction

At present CFD become one of the major instruments of aerodynamic analysis and design. The main challenge to investigators in this field is a prediction of separated flow characteristics. Separated flows commonly encountered at take-off and landing regimes of aircraft flight and sometimes at cruise ones, and their numerical investigations are of great practical interest.

There exist two major approaches to numerical investigations of viscous flows at high Reynolds numbers, including possible separation regions. The most general approach considers numerical solution of time-averaged Navier-Stokes equations using an adequate turbulence model. This approach makes it possible to take into account all complex flow phenomena. However, it requires rather great computer capacities. Moreover, possible imperfection of available turbulence models used in the calculations do not always yield results that are in good agreement with the experiment.

The second approach is based on the solution of the viscous-inviscid flow interaction problem (zonal approach). In accordance with it the flow region at high Reynolds numbers can be divided into two parts: an inviscid part where the Euler equations or some approximation of them are to be solved and a viscous one (boundary layers and wakes) in which the time-averaged Navier-Stokes equations can be considerably simplified owing to a small layer thickness (the Prandtl boundary layer equations). These external (inviscid) and internal (viscous) solutions should be matched and the problem of organization of convergent iterative procedure of their matching (viscous-inviscid interaction problem) is the central problem in this approach. First investigations in[1-3] followed by numerous works of other researchers showed a possibility of calculation of viscous flows including separated ones in the frames of this approach. Much fewer requirements for computer capacities as compared with the methods of direct solution of the Navier-Stokes equations have motivated a speedy development of viscous-inviscid interaction methods. Many researchers indicate that the accuracy of the methods based on the solution of the Navier-Stokes equations do not, so far, exceed that of the zonal methods.

The present paper considers the application of viscous-inviscid interaction methods to calculate both attached and separated flows over airfoils and high-lift systems.

Governing equations

Let consider a viscous compressible fluid flow at high Reynolds numbers. The viscous effects are known to be considerable only within

a wall and wake layers of small thickness δ. The flow in these layers is mainly turbulent. The flow governed by the time-averaged Navier-Stokes equations will be referred as a "Real Viscous Flow" (RVF). Following[1-2] let us introduce a so-called "Equivalent Inviscid Flow" (EIF) governed by the inviscid Euler equations. The boundary conditions on the surface of the body and on the wake centerline for EIF are chosen from the condition of coincidence of RVF and EIF parameters outside the viscous layer of thickness δ. Integration of the difference between EIF and RVF equations along normal to the surface across the viscous layer yields[2]:

$$v_{iw} = \frac{1}{\rho_{iw}} \frac{d}{ds}(\rho_{iw} u_{iw} \delta^*);$$

$$\frac{d\theta}{ds} + (H + 2 - M_e^2)\frac{\theta}{u_{iw}}\frac{du_{iw}}{ds} = \frac{1}{2}c_f +$$

$$+k_w(\theta_n + c_\tau) +$$

$$+\frac{1}{\rho_{iw} u_{iw}^2}\frac{d}{ds}\left[\int_0^\delta (p - p_i)dn + \int_0^\delta \rho\overline{u'^2}dn\right] =$$

$$= \frac{1}{2}c_f + E_1;$$

$$\frac{p_{iw} - p_w}{\rho_{iw} u_{iw}^2} = k_w(\theta + \delta^*) +$$

$$+\frac{1}{\rho_{iw} u_{iw}^2}\frac{d}{ds}(\rho_{iw} u_{iw}^2 \theta_n) - \left(\frac{v_{iw}}{u_{iw}}\right)^2 +$$

$$+\frac{k_w}{\rho_{iw} u_{iw}^2}\int_0^\delta (p_i - p)dn - \frac{k_w}{\rho_{iw} u_{iw}^2}\int_0^\delta \rho\overline{u'^2}dn +$$

$$+\frac{1}{\rho_{iw} u_{iw}^2}\frac{d}{ds}\int_0^\delta -\rho\overline{u'v'}dn = k^*(\theta + \delta^*) + E_2,$$

where the following notations are introduced: s and n - coordinates along the surface and normal to it, u and v - tangential and normal to the surface velocity components, ρ - density, p - pressure, M - Mach number, c_f - skin friction coefficient, u' and v' - fluctuational velocity components, k_w - surface curvature, subscript i means EIF values, subscript w - values at the surface, e - values at the outer edge of the boundary layer, and

$$\delta^* = \frac{1}{\rho_{iw} u_{iw}}\int_0^\delta (\rho_i u_i - \rho u)dn;$$

$$\theta = \frac{1}{\rho_{iw} u_{iw}^2}\int_0^\delta [\rho u(u_{iw} - u) -$$

$$-\rho_i u_i (u_{iw} - u)]dn;$$

$$\theta_n = \frac{1}{\rho_{iw} u_{iw}^2}\int_0^\delta (\rho_i u_i v_i - \rho u v)dn;$$

$$c_\tau = \int_0^\delta \frac{(-\rho\overline{u'v'})}{\rho_{iw} u_{iw}^2}dn;$$

$$H = \frac{\delta^*}{\theta}; \quad k^* = k_w + \frac{d^2\delta^*}{ds^2}.$$

It is shown in[2] that the terms E_1 and E_2 are small both for the attached and separated boundary layers and could be neglected. Thus, the following set of equations is obtained:

$$v_{iw} = \frac{1}{\rho_{iw}}\frac{d}{ds}(\rho_{iw} u_{iw} \delta^*) \qquad (1a)$$

$$\frac{d\theta}{ds} + (H + 2 - M_e^2)\frac{\theta}{u_{iw}}\frac{du_{iw}}{ds} - \frac{1}{2}c_f = 0 \qquad (1b)$$

$$p_{iw} - p_w = k^* \rho_{iw} u_{iw}^2 (\theta + \delta^*) \qquad (1c)$$

If we neglect variations in the tangential velocity component u and density ρ in the EIF and consider them to be constant and equal to their values at the outer edge of the boundary layer, values δ^* and θ become standard boundary layer displacement and momentum thicknesses respectively.

Now equations (1) can be interpreted as follows. Equation (1a) is the boundary condition for the normal velocity component in the EIF, and it means that sources must be distributed along the airfoil surface in order to move the streamline to the distance δ^* normal to the surface. Such approach was proposed by Lighthill[4] and was called "the method of equivalent sources". Equation (1b) is the standard integral momentum equation (von Karman equation) to be solved for determination of boundary layer parameters. Equation (1c) can be applied after the calculations are completed to determine the pressure at the surface in the RVF by known pressure in the EIF.

Equation (1b) should be added by closure relations, turbulence model in particular. Following[5] let us write down two additional equations: definition of entrainment coefficient

c_E, which characterizes the gas amount ejected by a viscous flow from the external inviscid flow

$$c_E = \frac{1}{\rho_e u_e}\frac{d}{ds}(\rho_e u_e H_1 \theta), \qquad (2)$$

where

$$H_1 = \frac{\delta - \delta^*}{\theta},$$

The second additional equation for entrainment coefficient is called "lag-entrainment equation":

$$\theta\frac{dc_E}{ds} = 2\left\{\frac{c_\tau}{dc_\tau / dc_E}\right\}\left\{\frac{a_1}{(u_m / u_e)(L/\delta)} \times \right.$$
$$\times\frac{c_{\tau EQo}^{1/2} - \lambda\, c_\tau^{1/2}}{H + H_1} + \left[\frac{\theta}{u_e}\frac{du_e}{ds}\right]_{EQ} - \qquad (3)$$
$$\left. -\frac{\theta}{u_e}\frac{du_e}{ds}\left[1 + 0.075M_e^2\left(\frac{1 + 0.2M_e^2}{1 + 0.1M_e^2}\right)\right]\right\}$$

Here subscript EQ corresponds to the equilibrium conditions corresponding to constant values of formparameter H and maximum shear stress coefficient c_τ, a_1 - turbulence structure parameter, L/δ - nondimensionalized dissipation length, u_m/u_e - ratio of longitudinal velocity at the point of maximum shear stress to the velocity at the outer edge of the boundary layer. Detailed description of these parameters and their relations with other boundary layer values can be found in[5]. This equation is in fact an integral equivalent of differential turbulence model of Bradshow[6] resulting from the turbulent kinetic energy equation.

So, the set of boundary layer equations includes integral momentum equation (1b), entrainment equation (2) and "lag-entrainment" equation (3). This set of equations must be closed by relations expressing values of formparameter H_1, friction coefficient c_f, equilibrium and nonequilibrium shear stress coefficients c_τ and $c_{\tau EQ}$ in terms of formparameter H and momentum thickness-based Reynolds number Re_θ. These relations are described below.

Special boundary conditions for EIF should be posed at the cut issuing from the airfoil trailing edge and representing the wake. The wake is artificially divided onto upper (subscript u) and lower (subscript l) parts each of them being a continuation of boundary layers from the upper and lower surfaces of the airfoil respectively. The modeling of the displacement wake effect in solving the EIF problem dictates that the normal velocity component jump on the cut (subscript c) should be as follows:

$$(\Delta v)_c = \frac{1}{\rho_{iu}}\frac{d}{ds}(\rho_{iu}u_{iu}\delta_u^*) + \frac{1}{\rho_{il}}\frac{d}{ds}(\rho_{il}u_{il}\delta_l^*) \qquad (4)$$

The viscous wake curvature leads to a tangential velocity component jump on the cut (wake centerline):

$$(\Delta u)_c = \frac{1}{2}k_c(u_{iu} + u_{il})(\theta_u + \theta_l + \delta_u^* + \delta_l^*) \qquad (5)$$

Thus, equations (1a), (4), and (5) represent boundary conditions for EIF problem with governing equations being the inviscid Euler equations or some approximation of them.

Viscous-inviscid interaction

Since the closing relations for the boundary layer are derived for an incompressible fluid, let, following[5] introduce a formparameter of an equivalent incompressible flow $\bar{H}$ which is related to H as follows:

$$H = (\bar{H} + 1)z - 1; \qquad z = 1 + 0.2M^2.$$

Equations (2) and (1a) can be rewritten as follows (subscript e is omitted):

$$c_E = -(H + 1)H_1 G + H_1\theta\frac{d\bar{H}}{ds} + \frac{1}{2}c_f H_1; \qquad (6)$$

$$\Sigma = -(H + 1)(H - 0.4M^2)G + z\theta\frac{d\bar{H}}{ds} + \frac{1}{2}c_f H; \qquad (7)$$

$$\Sigma = \frac{v}{u}; \qquad G = \frac{\theta}{u}\frac{du}{ds}; \qquad H_1' = \frac{dH_1}{d\bar{H}}$$

The curve $H_1(H)$ has its minimum in the vicinity of separation, $H_1'<0$ for an attached flow, $H_1'>0$ for a separated flow and $H_1'=0$ at a separation point. Thus, is possible to integrate (6) and determine the value of $\bar{H}$ in the "direct" mode with the specified distribution of u obtained from EIF only for attached flows. At the separation point the coefficient at the derivative of $\bar{H}$ becomes zero and integration fails. This result reflects the well-known Goldstein singularity at the separation and reattachment points that prevents integration of boundary layer equations with the specified velocity gradient. This singularity reveals itself only in the equation (2) of the set of boundary layer equations, the

rest two equations (1b) and (3) can be solved (and were solved both for attached and separated regions) with a specified value of velocity gradient from EIF. By excluding the velocity gradient from (6) and (7) it is possible to obtain the following form of equation for the derivative of $\bar{H}$:

$$\theta\frac{d\bar{H}}{ds}=\frac{[\Sigma H_1-(H-0.4M^2)c_E-0.2H_1M^2c_f]}{[H_1z-(H-0.4M^2)H_1^t]};(8)$$

This equation has no singularity at the separation point and should be solved with a specified value of source intensity coefficient Σ ("inverse" mode).

The boundary condition for EIF is obtained by exclusion of dH/ds from (6) and (7):

$$Tu\Sigma=Tv=P\frac{du}{ds}+Qu; \qquad (9)$$

$$T=\frac{H_1^t}{HH_1^t-H_1z};$$

$$P=-(H+1)(1-0.4M^2T)\theta;$$

$$Q=\frac{1}{2}c_f+\frac{c_Ez}{HH_1^t-H_1z}$$

This boundary condition links the value of the normal velocity component with the tangential velocity component ant its gradient. It is nonsingular everywhere and is used both for attached and separated flows. The difference in application of this boundary condition for attached and separated flows consists in that for preseparated and separated flows (H>1.4) both normal and tangential velocity components are taken at the current inviscid iteration (as unknowns), and for attached flow ($H\leq$1.4) the tangential velocity component is taken from previous iteration and in fact the value of normal velocity component is specified as the boundary condition.

Such an approach to the viscous-inviscid interaction is a variant of so-called "quasi-simultaneous" method. In the present approach some estimate of the boundary layer influence on the external flow (equation (9)) is added to the equations for external inviscid flow as a boundary condition. This approach was introduced in[7] and applied to calculation of subsonic flow about an airfoil. The term "quasi-simultaneous approach to viscous-inviscid interaction" was introduced in[8] where on the contrary some approximation of the effect of the external inviscid flow written in the form of Cauchy integral was added to the boundary layer equations.

The present paper deals with a mixed method of viscous-inviscid coupling. The direct method (calculation of the boundary layer equations with prescribed tangential velocity distribution) is used for a laminar boundary layer and an attached turbulent one (H<1.4). The quasi-simultaneous method given above (calculation of the equation (8) instead of (6) with prescribed distribution of source intensity Σ) is used for the rest part of the boundary layer. The laminar part of the boundary layer is calculated by the method[9] in parallel with the calculation of the laminar-turbulent transition point by the method of Granville[10].

Thus, the calculation procedure is the following: inviscid flow equations are solved with the boundary condition (9), the same boundary condition is satisfied on the wake, i.e. only displacement effect in the wake is taken into account. Values of functions T, P and Q in (9) are taken from the current solution of the boundary layer equations. Distributions of the tangential velocity u and source intensity Σ for the boundary layer equations are determined from the EIF solution. Laminar part of the boundary layer and thin part of the turbulent boundary layer are calculated in the "direct" mode with prescribed tangential velocity distribution. Then boundary layer equations (1b), (6) (considered as a differential equation for $\bar{H}$ and (3) are solved for the attached turbulent boundary layer while for the preseparated and separated turbulent boundary layer equation (8) is solved instead of (6).

Closure of boundary layer equations.

The set of boundary layer equations is closed by the following relations

$$\left.\begin{aligned} H_1&=H_1(\bar{H},\mathrm{Re}_\theta);\\ c_f&=c_f(\bar{H},\mathrm{Re}_\theta);\\ c_{E_{EQ0}}&=c_{E_{EQ0}}(\bar{H},\mathrm{Re}_\theta)\\ c_\tau&=c_\tau(\bar{H},\mathrm{Re}_\theta)\end{aligned}\right\} \qquad (10)$$

The first of these relations can be established based on the known velocity profile in the boundary layer. After a series of numerical experiments with various velocity profiles including that presenting separated ones with reverse flow, a universal relation was selected and used in calculations, namely

$$H_1 = \begin{cases} \dfrac{0.63H+1}{H-1}H + 0.75; & H < 2.61 \\ 7.27 + \dfrac{25.07}{H-0.42} - \dfrac{35.78}{H}; & H \geq 2.61 \end{cases}$$

The first branch of this relation is taken from[11], coefficients of the second branch are taken from the condition of smooth matching at the point H=2.61 up to the second derivative and from the results of numerical experiments. Relation for skin friction coefficient is taken from[12] and has the form

$$c_f = \frac{0.3e^{-1.33H}}{(\log R_\theta)^{1.74+0.31H}} + \\ +0.00011\left[\tanh(4 - 1.143H) - 1\right]$$

Relations (10) as well as values of parameters a_1, L/δ, u_m/u_e for separated boundary layer are also taken from[11]. More detailed description of the method is given in [13].

Calculation of inviscid flow over airfoils and high-lift systems.

The approach described above was applied to the calculation of transonic flow about single airfoils (computer code VISTRAN) and subsonic flow about multi-element airfoils (high-lift systems, computer code MULTIVIS).

The external inviscid transonic flow about an airfoil is described using a modified potential model. A conservative rotated finite-difference scheme[14] is used for a numerical solution of the potential equation. An approximate account for an entropy variation on a shock and a vorticity behind shocks using the Clebsch transformation[15] is introduced. Calculations are performed using an O-type grid generated by conformal mapping. A set of unknowns includes values of potential at the grid nodes plus the source intensities at the airfoil surface.

The external inviscid subsonic flow about multi-element airfoils is calculated using a panel method of symmetric singularities when each panel is characterized by a constant source and linearly varying vortex distributions. The singularity intensities are symmetric about the airfoil chords and are found from the boundary condition (9) satisfied at the center of each panel on the airfoil surfaces and in the wakes. The tangential velocity gradient is calculated using an equation of irrotationality

$$\frac{\partial u}{\partial s} = -k_w v_0 - \frac{\partial v_0}{\partial n}$$

where k_w is the surface curvature, subscript 0 denotes the velocity value less the contribution of the panel itself.

Correct account of wake influence, their shapes in particular for multi-element airfoils is much more important from the accuracy point of view than for single airfoils. The wake shapes are calculated by a construction of streamlines leaving the trailing edges. The wakes' lengths are equal to 4 chords of the largest element and there are 100 panels on each of them. Only wake displacement effect is taken into account.

Results for single airfoils and comparison with experimental data.

NACA64A010 airfoil

The experimental data for this airfoil are taken from[16]. The laminar-turbulent transition was fixed at 6.1% on the upper and lower surfaces. Fig.1 compares the experimental and calculated pressure distributions for M=0.8, Re=2×10^6, α=6.2°. The flow in this condition is characterized by a strong shock at $\bar{x}$=40% with a subsequent massive shock-induced separation which is detected in calculations.

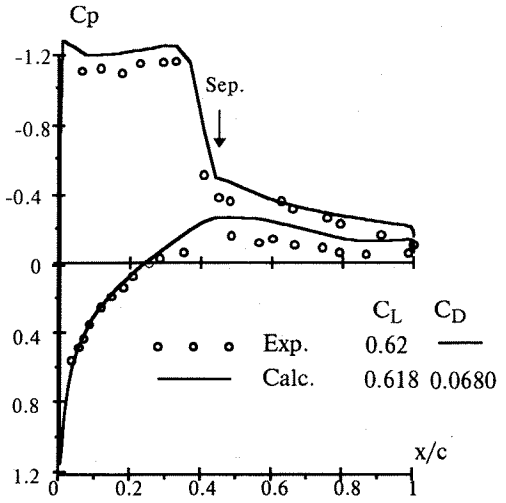

Fig.1. NACA64A010 airfoil, M=0.8, Re=2×10^6, α=6.2°.

GA(W)-1 airfoil.

Fig.2 shows a comparison of calculated and experimental total aerodynamic characteristics for a GA(W)-1 airfoil ($\bar{c}$=17%, M=0.15, Re=6.3×10^6) with a transition fixed at 7.5% on both surfaces[17]. The figure shows a good agreement of lift $c_L(\alpha)$ and pitching moment $c_M(\alpha)$ (relative to the airfoil leading edge) curves up to the maximum lift. As a whole, the calculated drag polar agrees well with the experimental one but it is slightly shifted to the left (Δc_{D0}=0.0017), what can be explained by inadequate consideration of the turbulence strip drag.

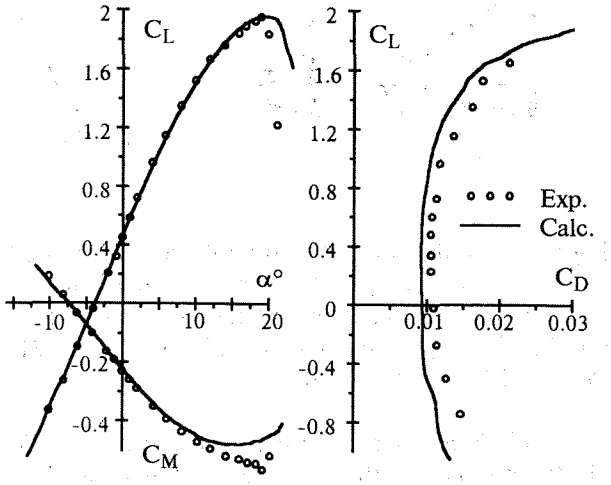

Fig.2. GA(W)-1 airfoil, M=0.15, Re=6.3×10^6.

NACA0012 airfoil.

This symmetric 12%-airfoil commonly used to verify calculation programs. Fig.3. presents a comparison of experimental[18] and calculated pressure distributions for a severe test case M=0.55, Re=9×10^6, α=9.86° (corrected to the wind tunnel interference value α=8.34°) with a transition fixed on both surfaces at 5%. In this case the flow features a developed forward supersonic zone terminated by a high-intensity shock. The calculation reveals a shock-induced separation at 14% with a subsequent attachment at 28% and a weak rear separation at 94%.

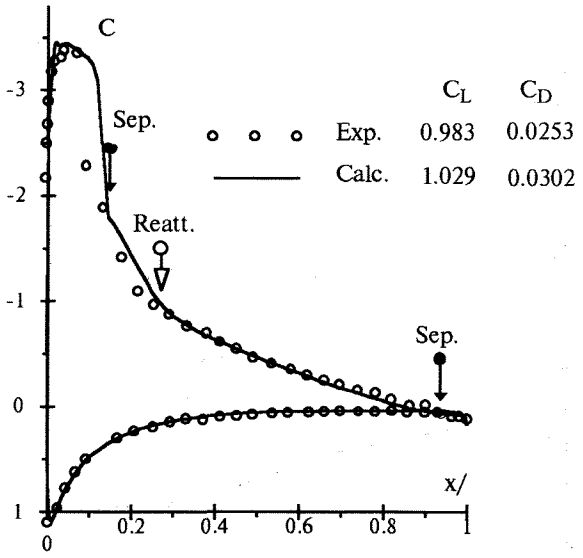

Fig.3. NACA0012 airfoil, M=0.55, Re=9×10^6, α=8.34° (α_{exp}=9.86°).

Fig.4 compares the experimental[19] and calculated maximum lift values vs. Reynolds and Mach numbers, as well as the value of the lift curve slope vs. Mach number and drag coefficient at α=0 vs. Mach number. It is seen that the calculation data represent adequately the test results in a wide range of Mach and Reynolds numbers.

Results for high-lift airfoils and comparison with experimental data.

Fig.5 illustrates the results of calculation of the flow about an airfoil and a flap. Calculations are performed for a GA(W)-1 airfoil with a 29%-chord Fowler flap at M=0.21, Re=2.2×10^6, α=10°, angle of the flap deflection δ_f=40°. A streamline pattern, separated regions, boundary layer velocity profiles at several stations and comparison of calculated and experimental pressure distributions are presented in the Figure.

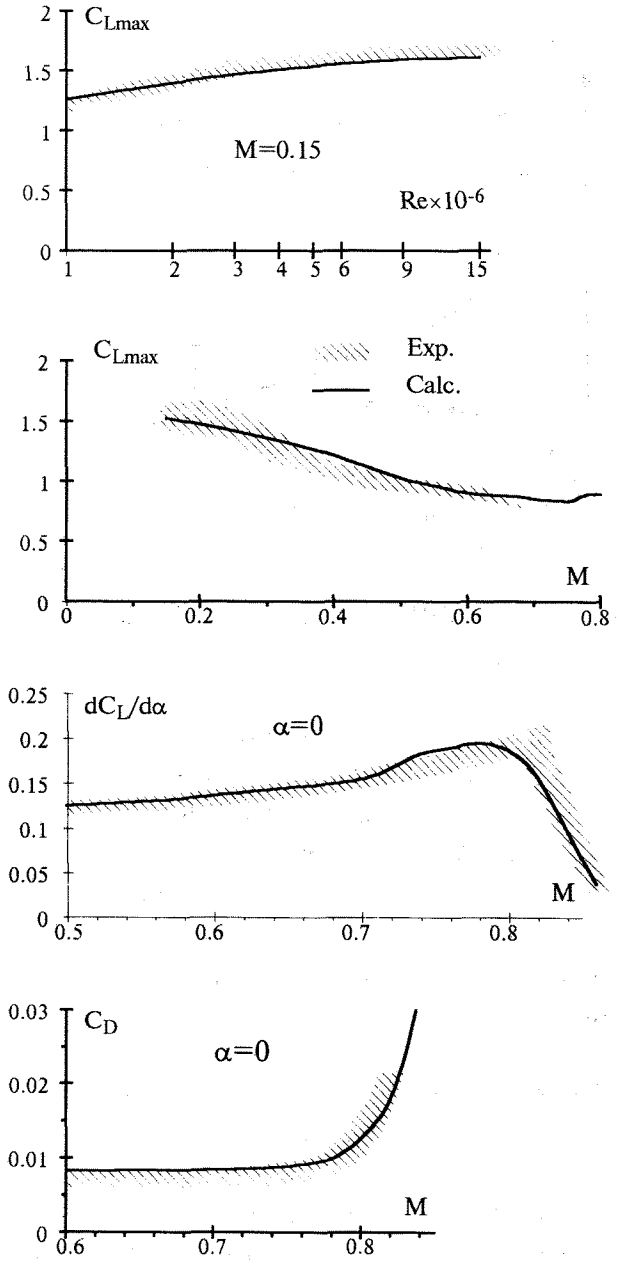

Fig.4. Comparison of experimental and calculated maximum lift, lift curve slope and drag for the NACA0012 airfoil.

The experiment pressure distribution is taken from[20]. The present case corresponds to a maximum lift of this configuration. This case is characterized by the presence of a small separated region at the rear part of the flap and a massive separation in the wake of the main airfoil. Such wake separation regions, that are absent in the flows about single airfoils, are typical for flows about high-lift systems and their influence constitutes the main reason of importance of accurate wake calculation for multi-element airfoils. Separation zones could be identified by the reverse flow regions that could be seen on the plots of velocity profiles at stations *A*, *B* and *C*. The agreement of calculated and experimental pressure distributions is quite satisfactory.

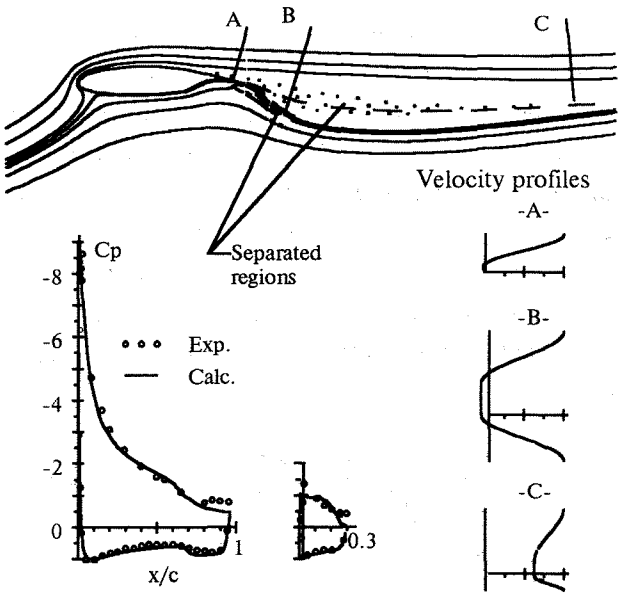

Fig.5. Calculation of streamlines, separated regions, velocity profiles and comparison of experimental and calculated pressure distributions for the GA(W)-1 airfoil with 29% flap, M=0.21, Re=2.2×10^6, α=10°, δ_f=40°.

Fig.6 compares the calculated lift vs. angle of attack curves with the experimental data of[21] for a 30%-flap at M=0.13, Re=2.2×10^6 and flap angles δ_f=10, 20, 30 and 40°. In order to simplify the calculation procedure, the main element cove was slightly smoothed. The calculation shows good agreement with the experiment at δ_f=10, 20 and 30° up to the maximum lift. At δ_f=10°, it is impossible to determine a correct critical angle of attack because the test points are scarce.

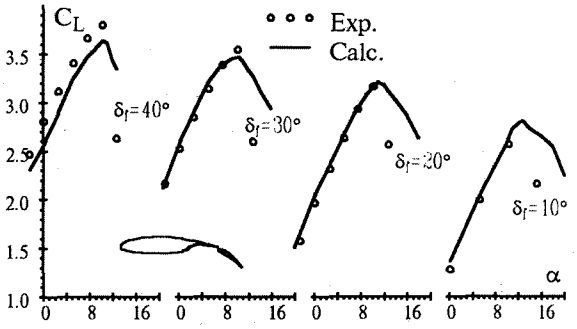

Fig.6. Lift curves for the GA(W)-1 airfoil with 30%-flap at M=0.13, Re=2.2×10^6.

One more example of total aerodynamic characteristics calculation of an airfoil with slat is given in Fig.7 for M=0.201, Re=2.83×10^6, slat deflection angle, δ_s=43.9°. Lift curve vs. angle of attack, drag polar and pitching moment (with respect to one-quarter chord of the main element) vs. lift coefficient are presented at this Figure. Total aerodynamic characteristics compare reasonably well with the experimental ones taken from[22] except for drag at low lift coefficient what is attributed to the separation on the lower surface of the slat not taken into account in the calculations.

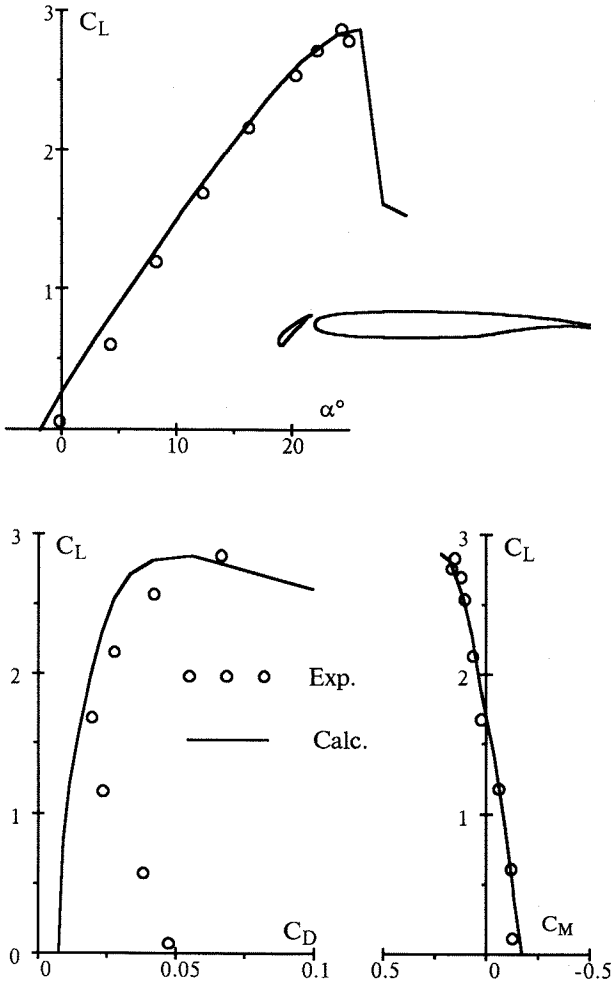

Fig.7. Total aerodynamic characteristics of an airfoil with slat at M=0.201, Re=2.83×10^6, δ_s=43.9°.

And finally, an example of calculation of total aerodynamic characteristics for a four-element high-lift system at M=0.201, Re=2.83×10^6, δ_s=47.2°, δ_{f1}=30° (deflecton of the first section of the flap), δ_{f2}=49.7° (deflecton of the second section of the flap) is presented at Fig.8. The calculated characteristics are the same as presented in the previous Figure. The calculated results show satisfactory agreement with the experiment again except for drag values at low lift coefficient values what could be also explained by the lack of account of the separation on the lower surface of the slat.

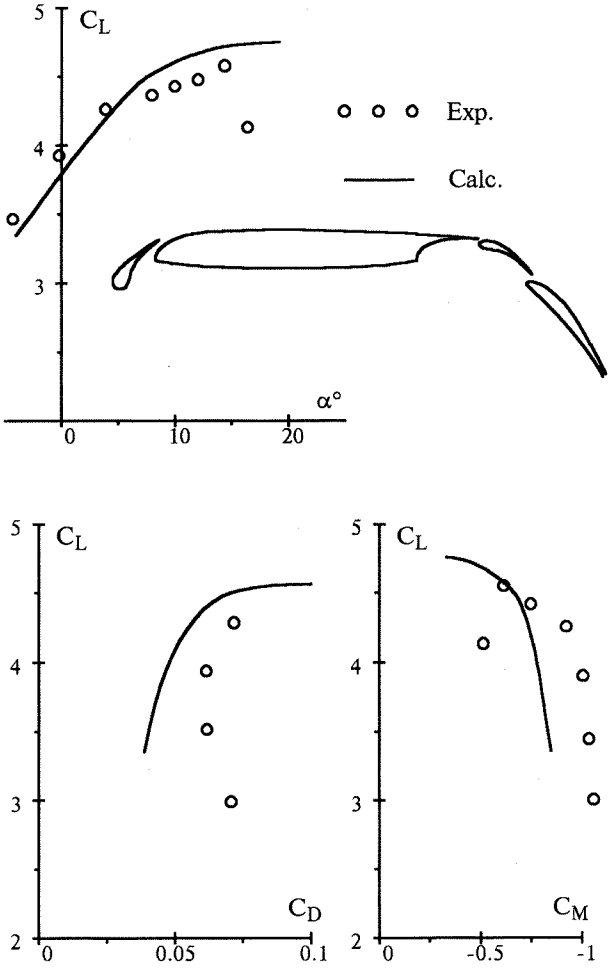

Fig.8. Total aerodynamic characteristics of the four-element high-lift system at M=0.201, Re=2.83×10^6, δ_s=47.2°, δ_{f1}=30°, δ_{f2}=49.7°.

Conclusions

A method is considered for calculation of steady attached and separated 2D flows. The method is based on viscous-inviscid interaction model. A quasi-simultaneous approach to viscous-inviscid coupling is used when some relationship between normal and tangential velocity and its longitudinal derivative is used as a boundary condition for an inviscid flow in the preseparated and separated regions. A standard boundary condition on the normal velocity value is used for attached regions. This approach was proved to be rapidly convergent both for attached and separated flows.

The method is applied to calculation of a transonic flow about a single airfoil (computer code VISTRAN) and a subsonic flow about a multi-element airfoil (high-lift system, computer code MULTIVIS). Calculation of outer (inviscid) flow with boundary conditions mentioned above is carried out by singularity method for low speeds (multi-element airfoil) or by a solution of a modified transonic potential equation for high subsonic speeds (single airfoil). In the last case the modification of potential equation permits the vorticity behind the shock to be taken into account. Inner (viscous) flow is governed by laminar and turbulent boundary layer equations in an integral form. In the regions of preseparated and separated flow these equations are solved in an inverse mode in order to avoid the Goldstein singularity at the separation and reattachment points.

Comparisons of calculated results with well-established experimental results both for single and multi-element cases showed good agreement including determination of maximum lift and its dependence on Mach and Reynolds numbers as well as on flap deflection for high-lift systems.

References

1. J.C.Le Balleur. Strong Matching Method for Computing Transonic Viscous Flows Including Wakes and Separations. La Recherche Aerospatiale, No.3,pp.21-45,1981.
2. R.C.Lock, M.C.P.Firmin. Survey of Techniques for Estimating Viscous Effects in External Aerodynamics. Proc. of IMA Conference on Numerical Methods in Aeronautical Fluid Dynamics, March 30 - Apr. 1, 1981, in P.Roe (Ed.), Academic Press, 1983.
3. L.B.Wigton, M.Holt. Viscous-Inviscid Interaction in Transonic Flow. AIAA Paper, 81-1003, 1981.
4. M.J.Lighthill. On Displacement Thickness. J. Fluid Mech., vol.4, pp.383-392, 1958.
5. J.E.Green, D.J.Weeks, J.W.F.Brooman. Prediction of Turbulent Boundary Layers and Wakes in Compressible Flow by a Lag-Entrainment Method. RAE TR 72231 (ARC-RM 3791), 1977.
6. P.Bradshow. Turbulence. Springer-Verlag, Berlin, Heidelberg, New York, 1978.
7. A.G.T.Cross. Boundary Layer Calculation and Viscous-Inviscid Coupling. ICAS-86-2.4.1, 1986.
8. A.E.P.Veldman. New Quasi-Simultaneous Method to Calculate Interacting Boundary Layers. AIAA J., vol.19, pp.79-85, 1981.
9. C.B.Cohen, E.Reshotko. Similar Solution for the Compressible Laminar Boundary Layer. NACA Rep. 1294, 1956.
10. H.Schlichting. Boundary Layer Theory. McGraw-Hill, New York, 1960.
11. R.E.Melnik, J.W.Brook. The Computation of Viscous-Inviscid Interaction on Airfoils with Separated Flow. Numerical and Physical Aspects of Aerodynamic Flows III, New York, 1986.
12. T.W.Swafford. Analytical Approximation of Two-Dimensional Separated Turbulent Boundary-Layer Velocity Profiles. AIAA J., vol.6, No.21, 1983.
13. A.V.Wolkov, S.V.Lyapunov. Numerical Prediction of Transonic Viscous Separated Flow Past an Airfoil. Theoret. and Comp. Fluid Dyn., vol.6, No.1, pp.49-63, 1994.
14. A.Jameson. Acceleration of Transonic Potential Calculations on Arbitrary Meshes by the Multiple Grid Method. AIAA Paper 79-1458, 1979.
15. S.V.Lyapunov. Accelerated Method of the Euler Equation Solution in Transonic Airfoil Flow Problem. ICAS-92-4.2.3, 1992.
16. D.A.Johnson, W.D.Bachalo. Transonic Flow Past a Symmetric Airfoil: Inviscid and Turbulent Flow Properties. AIAA J., vol.183, pp.16-24, 1980.
17. R.J.McGhee, W.D.Beasley. Effects of Thickness on the Aerodynamic Characteristics of an Initial Low-Speed Family of Airfoils. NASA TM-X-72843, 1976.
18. C.D.Harris. Two-Dimensional Aerodynamic Characteristics of the NACA0012 Airfoil in the Langley 8-foot Transonic Pressure Tunnel. NASA TM 81927, 1981.
19. W.J.McCroskey. A Critical Assessment of Wind Tunnel Results for the NACA0012 Airfoil. AGARD Symposium on Aerodynamic Data Accuracy and Quality: Requirements and Capabilities in Wind Tunnel Testing, AGARD CP 429, Paper 1, Sept.28-Oct.2, 1987.
20. W.H.Wentz, H.C.Seetharam. Development of a Fowler Flap System for a High Performance General Aviation Airfoil. NASA CR-2443, 1974.
21. W.H.Wentz, H.C.Seetharam, K.A.Fiscko. Force and Pressure Tests of the GA(W)-1 Airfoil with a 30% Fowler Flap. NASA CR-2833, 1977.
22.E.Omar, T.Zierten, M.Hahn, E.Szpiro, A.Mahal. Two-Dimensional Wind-Tunnel Tests of a NASA Supercritical Airfoil with Various High-Lift Systems: VolumeII - Test Data. NASA CR-2215, 1973.